NASA TECHNICAL NOTE

NASA TN D-3138

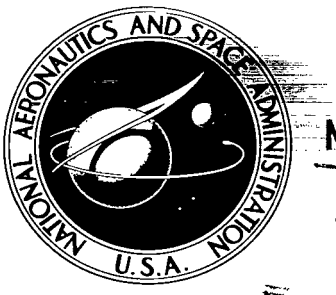

EFFECTS OF A MOMENTUM BUFFER REGION ON THE COAXIAL FLOW OF DISSIMILAR GASES

by Robert G. Ragsdale

Lewis Research Center
Cleveland, Ohio

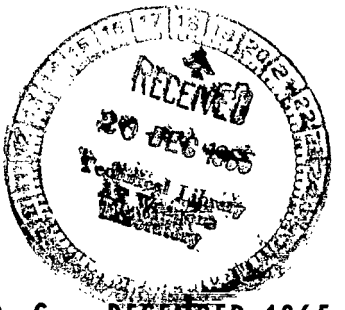

NATIONAL AERONAUTICS AND SPACE ADMINISTRATION - WASHINGTON, D. C. - DECEMBER 1965

NASA TN D-3138

EFFECTS OF A MOMENTUM BUFFER REGION ON THE COAXIAL FLOW OF DISSIMILAR GASES

By Robert G. Ragsdale

Lewis Research Center
Cleveland, Ohio

NATIONAL AERONAUTICS AND SPACE ADMINISTRATION

For sale by the Clearinghouse for Federal Scientific and Technical Information
Springfield, Virginia 22151 – Price $1.00

EFFECTS OF A MOMENTUM BUFFER REGION ON THE COAXIAL FLOW OF DISSIMILAR GASES*

by Robert G. Ragsdale

Lewis Research Center

SUMMARY

An analytical study was made of the isothermal mass and momentum transfer that occurs when a heavy, slow-moving gas is injected coaxially into a duct of light, fast-moving gas. The outer stream is composed of two regions: an outermost region moving at high velocity, and an annular sheath of intermediate velocity that is immediately adjacent to the central core, or jet, inner fluid. As a basis for comparison, the total mass flow rate of outer fluid is held constant; thus, as the buffer region velocity is decreased, the velocity of the remaining outer region is increased. The effects of the velocity and thickness of this buffer region on the mixing of the two fluids are investigated for both laminar and turbulent flow.

Outer- to inner-fluid initial-velocity ratios of 10, 50, and 100 are considered. Some representative velocity and concentration fields are shown for laminar and turbulent flow. The effect of a momentum buffer region is presented in terms of the amount of inner stream fluid that is contained within a specified length of the outer duct. The diameter of the duct is taken to be four times that of the initial jet; duct lengths of 2 and 4 jet initial diameters are considered.

In a gaseous-fuel nuclear rocket engine, stream mixing is undesirable because it tends to dilute the central core of fissionable gas with the surrounding hydrogen propellant, and thus leads to an increase in required reactor pressure in order to maintain criticality. The results of this study show that "optimum" values of both buffer velocity and thickness exist which give a maximum amount of inner fluid in a given length of duct. The optimum velocity is greater for turbulent flow than for laminar flow. The optimum buffer thickness was found to be relatively independent of whether the flow is laminar or turbulent. For the system studied, the optimum buffer thickness is about 1 inner stream radius. The presence of a buffer region increases the amount of inner gas contained in a duct length of 2 initial jet diameters by more than a factor of 2.

---

*Presented at the AIAA Propulsion Joint Specialists Conference, Colorado Springs, Colorado, June 14-18, 1965.

INTRODUCTION

The interaction between two coaxially flowing fluids is a subject of considerable interest, both academic and practical. A description of mass, momentum, and energy transfer between dissimilar coaxial streams is required in order to understand and design combustion chambers, jet pumps and ejectors, and afterburners. Recent experimental and anlytical studies have been reported that directly involve such a flow pattern. In a supersonic combustor (refs. 1 to 4) a hydrogen jet is injected into a coflowing stream of oxidizer gas. In a proposed concept for a nuclear rocket engine (refs. 5 to 7) a low-velocity, fissionable gas is injected into a coaxially flowing, high-velocity stream of hydrogen propellant. In both situations, the goal of the studies is to understand, to predict, and, ultimately, to influence the mixing rate of the two species.

For the gaseous-fueled-reactor concept, the mixing is undesirable, because it tends to dilute the nuclear fuel with hydrogen and thus leads to an increase in required reactor pressure. Flow schemes that result in slower stream mixing are therefore of interest. Since the mixing occurs primarily because the outer stream velocity greatly exceeds that of the inner stream, it is possible, in principle, to delay the interaction of the two streams by separating them by means of a buffer region of fluid flowing at some intermediate velocity. This report describes an analytical study of the characteristics of such a flow field.

In particular, the system to be considered is one in which a jet of low-velocity, heavy gas is separated from a surrounding, high-velocity, light gas by an annular sheath of intermediate-velocity, light gas. The gases are contained within a duct as illustrated in figure 1. The situation considered is one in which the total mass flow rate of the light gas is held constant as it might be in a rocket engine that is required to produce a certain amount of thrust. Thus, as the velocity of the buffer region is reduced, the velocity of the remaining outer stream must be increased to maintain a constant mass flow rate.

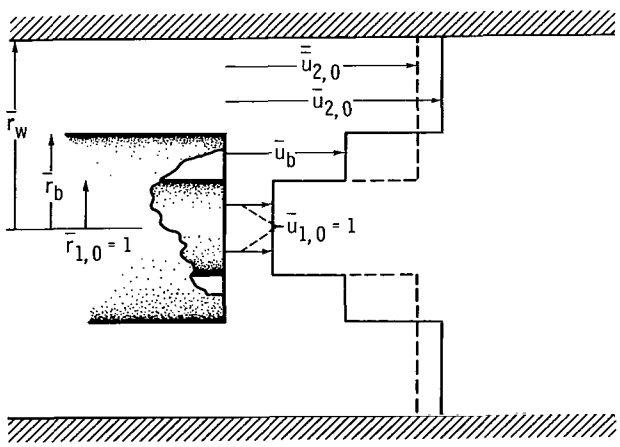

Figure 1. - Calculation model.

The numerical solution of reference 5 and its extension to turbulent flow (ref. 7) have been used to investigate the effects of a momentum buffer region on the coaxial mixing of dissimilar gases for isothermal flow. The primary parameters are the buffer region thickness and velocity. Calculations were carried out for both laminar and turbulent flow. Three values of average outer- to inner-

stream velocity ratio were considered. The results are compared with the case where no buffer region is present. The results presented indicate that a momentum buffer region can be used to alter significantly the rate of mixing near the injection point of a coaxial jet.

SYMBOLS

b	width of mixing region, ft
c	concentration of inner stream species, mole fraction
D	dimensional diffusion coefficient, ft^2/sec
$\overline{D}$	dimensionless diffusion coefficient
$D_{1,1}$	molecular self-diffusion coefficient of species 1, ft^2/sec
$D_{1,2}$	binary diffusion coefficient of species 1 and 2, ft^2/sec
K	constant
M	molecular weight, lb/lb mole
$Re_{1,0}$	initial Reynolds number of inner stream, $2r_{1,0}u_{1,0}\rho_{1,0}/\mu_{1,0}$
r	radial coordinate, ft
$\overline{r}$	dimensionless radius, $r/r_{1,0}$
$Sc_{1,0}$	initial Schmidt number of species 1, $\mu_{1,0}/\rho_{1,0}D_{1,1}$
u	axial velocity, ft/sec
$\overline{u}$	dimensionless axial velocity, $u/u_{1,0}$
$\overline{V}_2$	molecular volume ratio
v	radial velocity, ft/sec
$\overline{v}$	dimensionless radial velocity, $v/u_{1,0}$
z	axial coordinate, ft
$\overline{z}$	dimensionless axial position, $z/r_{1,0}$
β	molecular weight parameter, $(M_1/M_2) - 1$
ϵ	eddy diffusivity, ft^2/sec
ϵ^+	dimensionless eddy viscosity, $\rho\epsilon/\mu$
η_b	normalized containment factor

η_c containment factor

μ local viscosity

$\overline{\mu}$ dimensionless viscosity

ρ density, lb/ft^3

ψ stream function (see eqs. (5) and (6))

Subscripts:

av average

b buffer

cℓ centerline

max maximum

min minimum

t total

w wall

0 injection point (z = 0)

1 inner stream species

2 outer stream species

Superscripts:

$\overline{\ }$ dimensionless quantity

$=$ average over entire outer fluid region

ANALYTICAL METHOD

The basic analytical method used was reported in reference 5 for laminar flow and is extended to turbulent flow in references 6 and 7. It will be briefly reiterated here, along with a more detailed discussion of its application to a turbulent three-region system.

Laminar Flow

The steady-state boundary-layer equations for isothermal, constant pressure, axisymmetric flow are

Continuity:

$$\frac{\partial}{\partial r}(\rho v r) + \frac{\partial}{\partial z}(\rho u r) = 0 \tag{1}$$

Momentum:

$$v\frac{\partial u}{\partial r} + u\frac{\partial u}{\partial z} = \frac{1}{\rho r}\frac{\partial}{\partial r}\left(r\mu\frac{\partial u}{\partial r}\right) \tag{2}$$

Diffusion:

$$v\frac{\partial c}{\partial r} + u\frac{\partial c}{\partial z} = \frac{\rho}{r}\frac{\partial}{\partial r}\left(\frac{rD_{1,2}}{\rho}\frac{\partial c}{\partial r}\right) \tag{3}$$

It is assumed that there are no significant pressure gradients due to friction or momentum transfer. The dimensional equations (1), (2), and (3) are made nondimensional by normalizing all quantities to a dimensionally similar quantity in the inner stream at the injection point. For example, the dimensionless viscosity $\bar{\mu}$ is the ratio of local viscosity to that of pure inner stream fluid $\mu/\mu_{1,0}$; the axial velocity is normalized to the jet injection velocity so that $\bar{u} = u/u_{1,0}$; and the axial position and radius are normalized to the jet radius, so that $\bar{z} = z/r_{1,0}$ and $\bar{r} = r/r_{1,0}$. The dimensionless diffusion coefficient is given by $\bar{D} = (D_{1,2}/D_{1,1})$, where $D_{1,1}$ is the self-diffusion coefficient of the inner stream fluid.

The dimensionless continuity equation is now

$$\frac{\partial}{\partial \bar{r}}\left[\bar{r}\bar{v}\,(\beta c + 1)\right] + \frac{\partial}{\partial \bar{z}}\left[\bar{r}\bar{u}(\beta c + 1)\right] = 0 \tag{4}$$

where $\beta \equiv (M_1/M_2) - 1$. The system of equations is transformed from the $\bar{r}, \bar{z}$-plane to the $\psi, \bar{z}$-plane, where the stream function ψ satisfies the continuity equation (eq. (4)):

$$\frac{\partial \psi}{\partial \bar{z}} = -(\bar{r}\bar{v})(\beta c + 1) \tag{5}$$

$$\frac{\partial \psi}{\partial \bar{r}} = (\bar{r}\bar{u})(\beta c + 1) \tag{6}$$

Introducing dimensionless quantities and the stream function along with the usual boundary-layer assumption that $\partial\psi/\partial\bar{z} << d\psi/\partial\bar{r}$ yields the following equation set:

$$\int_0^{\bar{r}} \bar{r}' \, d\bar{r}' = \int_0^{\psi} \frac{1}{\bar{u}(\beta c + 1)} \, d\psi' \tag{7}$$

$$\frac{\partial \bar{u}}{\partial \bar{z}} = 2 \frac{\beta + 1}{Re_{1,0}} \frac{\partial}{\partial \psi} \left[\bar{u} \bar{u} \bar{r}^2 (\beta c + 1) \frac{\partial \bar{u}}{\partial \psi} \right] \tag{8}$$

$$\frac{\partial c}{\partial \bar{z}} = \frac{2(\beta c + 1)}{Re_{1,0} Sc_{1,0}} \frac{\partial}{\partial \psi} \left[\bar{D} \bar{u} \bar{r}^2 \frac{\partial c}{\partial \psi} \right] \tag{9}$$

The boundary conditions are

$$\frac{\partial \bar{u}}{\partial \psi} = \frac{\partial c}{\partial \psi} = 0 \qquad \psi = 0$$

$$\bar{u}(\psi_{max}, \bar{z}) = \bar{u}_{2,0}$$

$$c(\psi_{max}, \bar{z}) = 0$$

The local dimensionless viscosity is calculated from a mixing law utilized in reference 5 that can be written in terms of dimensionless quantities as

$$\bar{\mu} = \frac{\beta c + 1}{(\beta + 1)c + \frac{1 - c}{\bar{\mu}_2}} \tag{10}$$

The dimensionless diffusion coefficient is obtained by writing the Gilliland Equation (ref. 8) in the form

$$\bar{D} \equiv \frac{D_{1,2}}{D_{1,1}} = \frac{2\sqrt{2(\beta + 2)}}{\left(1 + \bar{V}_2^{1/3}\right)^2} \tag{11}$$

where V_2 is the ratio of molecular volumes, as given in reference 8, of species 2 to species 1.

Equations (7) to (11) are solved numerically by a computer program (ref. 5) to obtain radial profiles of dimensionless velocity and concentration at specified axial positions downstream from the injection point. In addition to constants relating to the numerical integration scheme, the following inputs are necessary and sufficient to define a case:

(1) Physical properties: β, $\overline{\mu}_2$, $\overline{V}_2$, $Sc_{1,0}$

(2) Flow parameter: $Re_{1,0}$

(3) Initial velocity profile: $\overline{u}(0,\overline{r})$

(4) Initial concentration profile: $c(0,\overline{r})$

For all the cases discussed in this report, slug flow velocity profiles are used, as illustrated in figure 1 (p. 2). For concentration, the initial profile is

$$0 \leq \overline{r} \leq 1 \qquad c = 1$$

$$1 < r \leq r_{max} \qquad c = 0$$

With a buffer region, the initial velocity profile is

$$0 \leq \overline{r} \leq 1 \qquad \overline{u} = 1$$

$$1 < \overline{r} \leq \overline{r}_b \qquad \overline{u} = \overline{u}_b$$

$$\overline{r}_b < \overline{r} \leq \overline{r}_{max} \qquad \overline{u} = \overline{u}_{2,0}$$

and with no buffer region is

$$0 \leq \overline{r} \leq 1 \qquad \overline{u} = 1$$

$$1 < \overline{r} \leq \overline{r}_{max} \qquad \overline{u} = \overline{u}_{2,0}$$

Turbulent Flow

The laminar analysis is extended to include turbulent flow by adding turbulent transport coefficients to their molecular counterparts. Thus, the contribution of turbulence can be expressed in terms of a turbulent viscosity $\rho\epsilon$ and a turbulent diffusivity ϵ. It is also assumed that the eddy diffusivities for mass and momentum transfer are equal.

The total transport properties to be substituted in equations (2) and (3) in place of the laminar properties are written as

$$\mu_t = \mu + \rho\epsilon \tag{12}$$

$$D_t = D + \epsilon \tag{13}$$

A similar procedure is employed in references 1 to 3, where it is further assumed that $\rho\epsilon >> \mu$ and $\epsilon >> D$.

Assuming that the same mixing law as for equation (10) can be used to obtain a dimensionless total viscosity and diffusion coefficient in terms of a dimensionless eddy viscosity ϵ^+ results in

$$\overline{\mu}_t = \frac{\beta c + 1}{\dfrac{(\beta + 1)c}{1 + \epsilon^+} \dfrac{(1 - c)}{(1 + \epsilon^+)\overline{\mu}_2}} \tag{14}$$

$$\overline{D}_t = \frac{\beta c + 1}{\dfrac{(\beta + 1)c}{\overline{D} + \epsilon^+ Sc_{1,0}} + \dfrac{1 - c}{\overline{D} + \epsilon^+ \overline{\mu}_2 Sc_{1,0}(\beta + 1)}} \tag{15}$$

where

$$\epsilon^+ \equiv \frac{\rho\epsilon}{\mu}$$

The functional dependence of ϵ^+ remains to be specified in terms of spatial flow and/or property characteristics of the system. This has been accomplished in current coaxial mixing studies by utilizing Prandtl's postulate that in a region of free turbulence the eddy diffusivity is proportional to the width of the mixing region and to the velocity difference across it:

$$\epsilon = Kb(u_{max} - u_{min}) \tag{16}$$

This postulate and its application to single-component jets and wakes are discussed in reference 9.

The extension of equation (16) to variable-density systems can be achieved in different ways. It has been suggested that $\rho\epsilon$ is constant with radius (refs. 1 and 2) and

that the velocity difference should be replaced with $|\rho_2 u_2 - \rho_{c\ell} u_{c\ell}|$ (ref. 2). Reference 4 proposes that $\rho\epsilon$ is constant with radius and that a combination of mass flux ρu and momentum flux ρu^2 be employed. In reference 10 it is assumed that $\rho\epsilon/\mu$ is independent of radius, but dependent on axial position to some exponent. Reference 7 concludes that $\rho\epsilon/\mu$ can be taken as independent of radial and axial position and that the velocity difference should be expressed as $(|u_2/u_1 - 1|)^{1/2}$.

Although the various approaches have yielded unresolved differences, they all share some significant similarities. Each of these previous studies (1) report general agreement with some experimental data, (2) appear to be applicable for initial velocity ratios both above and below 1, (3) indicate that the radial variation of $\rho\epsilon$ is not significant, and (4) conclude that density ratio must be included as a parameter when applying equation (16) to variable-density systems. Each approximation has been shown to correlate data within certain ranges of flow and property parameters. This suggests that the difference between laminar and turbulent flow is much greater than the differences between the various algebraic descriptions of turbulent viscosity. The numerical solution of reference 5 and the turbulent viscosity expression of reference 7 have been used for the calculations reported herein because no linearization assumptions are required and because general agreement with average radial concentration data has been demonstrated (ref. 7) over the widest range of initial-velocity ratios ($0.83 \leq \bar{u}_2 \leq 0.97$, $1.25 \leq \bar{u}_2 \leq 49$).

A recent study (ref. 11) has shown that these various correlations predict about the same turbulent viscosity at the jet origin when they are compared at the same velocity ratio. It was also shown that, for nearly equal stream velocities, turbulent mixing can be reduced by the presence of honeycomb inserts to remove initial turbulence from the two streams just prior to the jet origin. The turbulent viscosity correlation of reference 7 used here included both the initial turbulence and that due to the shear between the two free streams.

From reference 7, the ratio of turbulent to laminar viscosity can be written as

$$\epsilon^+ \equiv \frac{\rho\epsilon}{\mu} = 0.12\left(\frac{\mu_1}{\mu_2}\right)\left(\frac{M_2}{M_1}\right)(\mathrm{Re}_{1,0} - 250)\left|\bar{u}_2 - 1\right|^{1/2} \tag{17}$$

For a two-region coaxial-flow situation, $\bar{u}_2$ is simply the ratio of outer to inner initial fluid velocity, and the use of equation (17) is straightforward. When a momentum buffer is present, there are two velocities in the outer fluid, and it must be assumed that equation (17) still applies, with some kind of an average velocity used to get an "effective" $\bar{u}_2$. It is not clear how to obtain one velocity to represent all of the outer fluid. Certainly this velocity should be some kind of average of the buffer region velocity

and the outer region velocity, but there are a number of possibilities, for example, a simple numerical average, a mass-flow-rate-weighted average, or a momentum-weighted average. The latter two procedures seem more realistic than a numerical average. For the most extreme case considered, the buffer region contained only 10 percent of the total mass flow of the outer fluid and 4 percent of the total momentum. Thus, either of the two weighted averaging methods produced a velocity that was essentially the same as that of the high-velocity outer region. The choice, then, was rather arbitrary; the $\bar{u}_2$ in equation (17) was evaluated with a momentum-weighted average velocity of the outer fluid.

SCHEDULE OF CALCULATIONS

The primary variables to be considered are the thickness of the buffer region, the velocity ratio in the buffer region, and the ratio of light-gas to heavy-gas initial velocity. Calculations were made for both laminar and turbulent flow.

The first of each series of cases was for no buffer region present. For example, an initial-velocity ratio of 10 was selected for the first case. For the next case, a buffer region thickness of 0.5 initial inner stream radius ($\bar{r}_b = 1.5$) was assigned, and the velocity ratio in this region was decreased until it was some specified fraction of that of the remaining outer fluid. A dimensionless channel radius $\bar{r}_w$ of 4 was assigned for all calculations, and as the buffer velocity was decreased, the velocity of the remaining outer fluid was increased to maintain a constant total-mass-flow rate of light gas. Thus, if the initial velocity ratio with no buffer region is $\bar{\bar{u}}_{2,0}$, then

$$\bar{\bar{u}}_{2,0}\left(\bar{r}_w^2 - 1\right) = \bar{u}_b\left(\bar{r}_b^2 - 1\right) + \bar{u}_{2,0}\left(\bar{r}_w^2 - \bar{r}_b^2\right) \tag{18}$$

For the illustrative case selected, $\bar{\bar{u}}_{2,0} = 10$ and $\bar{r}_b = 1.5$; for a buffer velocity that is 0.1 of the remaining outer fluid velocity,

$$\bar{u}_{2,0} = \frac{\bar{\bar{u}}_{2,0}\left(\bar{r}_w^2 - 1\right)}{\left(\frac{\bar{u}_b}{\bar{u}_{2,0}}\right)\left(\bar{r}_b^2 - 1\right) + \left(\bar{r}_w^2 - \bar{r}_b^2\right)} = 10.8$$

and $\bar{u}_b = 1.08$.

Average outer- to inner-velocity ratios of 10, 50, and 100 were considered. For each of these ratios, buffer- to outer-velocity ratios of 0.1, 0.2, 0.3, and 0.4 were

investigated. For all combinations of these variables, buffer thicknesses of 0.5 and 1 initial jet radius were calculated, as well as the situation of no buffer region. The following combinations were calculated for both laminar and turbulent flow:

Average outer- to inner-velocity ratio, $\bar{\bar{u}}_{2,0}$	10, 50, 100
Buffer- to outer-velocity ratio, $\bar{u}_b/\bar{u}_2$	0, 0.1, 0.2, 0.3, 0.4
Buffer region radius, $\bar{r}_b$	1, 1.5, 2.0

For all calculations, the following constant values were used: $\beta = 100$, $\bar{\mu}_2 = 0.2$, $\bar{V}_2 = 0.2$, and $Sc_{1,0} = 1.0$. As pointed out in references 5 and 10, the analytical results are relatively insensitive to the transport property ratios, so these choices are not critical. Therefore, the results of this study should be reasonably general and not restricted by the particular properties chosen. Some of the calculations performed for this study were repeated for molecular Schmidt numbers of 0.5 and 2, and the concentration and velocity profiles were virtually unaffected. Insensitivity of a similar analysis to Schmidt number was reported in reference 4. The laminar calculations are based on an inner stream Reynolds number of 200 and the turbulent cases for a Reynolds number of 20 000.

RESULTS AND DISCUSSION

The results of the calculations of three-region, two-component mixing will be presented in two main categories. First, detailed characteristics of concentration and velocity fields will be discussed for both laminar and turbulent flow. Second, a more generalized presentation of the effects of a buffer region will be made in terms of the total mass of inner stream fluid present in a channel of specified length.

Flow Field Characteristics

The general effect of a faster moving outer stream is to accelerate and dilute the inner stream fluid. This results from mass diffusion of the inner fluid radially outward into regions of higher velocity and also from acceleration of the inner fluid by momentum transfer radially inward. Figure 2(a) shows the concentration field for turbulent coaxial flow with an initial velocity ratio of 50. If the initial velocity ratio were lower than 50, the mixing of the two streams would occur more slowly. A buffer region of lower velocity immediately adjacent to the inner stream presents such a situation, at least initially.

Figure 2(b) shows the effect of reducing the velocity in a buffer region 1 jet radius

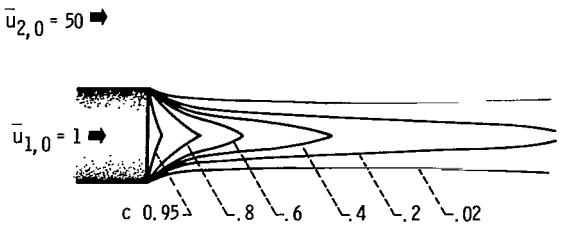

(a) No buffer region.

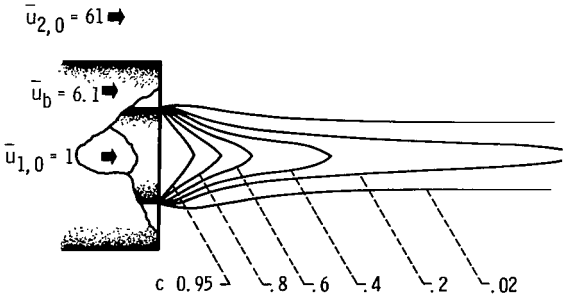

(b) Buffer thickness, 1; $\bar{u}_b/\bar{u}_{2,0} = 0.1$.

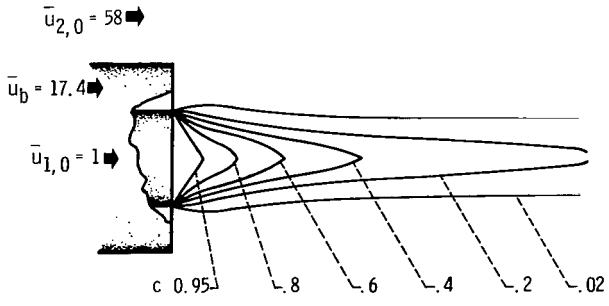

(c) Buffer thickness, 1; $\bar{u}_b/\bar{u}_{2,0} = 0.3$.

Figure 2. - Effect of buffer region on concentration field. Turbulent flow; $\bar{u}_{2,0} = 50$.

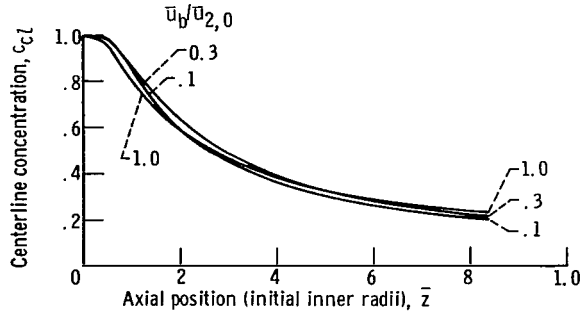

Figure 3. - Centerline concentration. Turbulent flow; $\bar{u}_{2,0} = 50$; buffer thickness, 1.

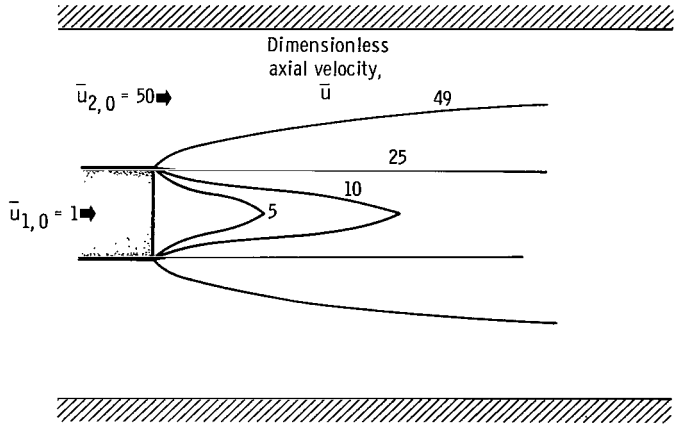

(a) No buffer region.

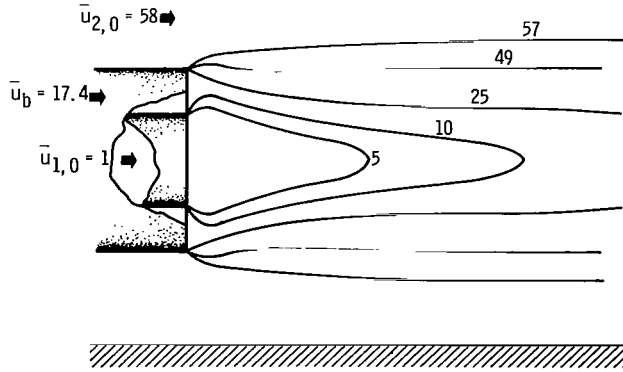

(b) Buffer thickness, 1; $\bar{u}_b/\bar{u}_{2,0} = 0.3$.

Figure 4. - Effect of buffer region on velocity field. Turbulent flow; $\bar{u}_{2,0} = 50$.

in thickness until it is 0. 1 that of the remaining outer stream. In order to maintain the same mass flow of outer fluid, or the same average velocity ratio of 50, the outer-fluid-velocity ratio between the buffer region and the channel $\bar{r}_w = 4$ is increased to 61 and the buffer-velocity ratio is then 6. 1. Figure 2(b) illustrates that the general effect of a momentum buffer is to reduce the mixing rate in the region near the jet. Farther downstream, the mixing zone produced by the shear between the high velocity outer flow and the slow moving buffer region penetrates to the inner zone and results in increased acceleration of the inner fluid.

Figure 2(c) shows the concentration field that results if the buffer- to outer-velocity ratio is increased from 0. 1 to 0. 3. Although the buffer velocity is higher, the mixing rate is less than for a buffer-velocity ratio of 0. 1. This indicates that there is an optimum buffer velocity and that buffer velocities below this value do not afford sufficient momentum in the buffer to offset the increased momentum in the outer stream required to maintain a constant mass flow. A comparison of the concentration lines $c = 0.6$ in figure 2 shows this effect.

Figure 3 is a plot of centerline concentration as a function of axial position for the three cases first discussed. The centerline concentration is slightly higher for a buffer-velocity ratio of 0. 1 for only 0. 5 jet radius downstream; beyond 2 radii downstream it falls a little below that for no buffer region. Between axial distances of 1 and 4. 5 jet radii, a buffer-velocity ratio of 0. 3 yields the highest centerline concentration. Figure 3 also serves to illustrate that centerline variations are relatively insensitive to effect of a buffer.

The effect of a buffer region on the velocity field is quite pronounced. This is shown

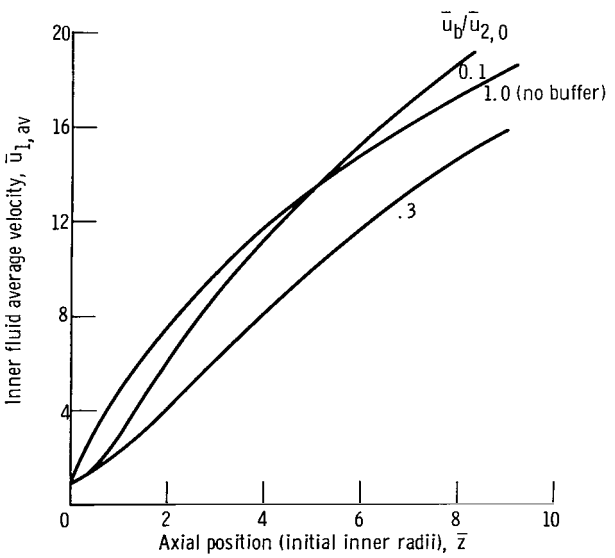

Figure 5. - Effect of buffer region on inner fluid average velocity. Turbulent flow; $\bar{u}_{2,0} = 50$; buffer thickness, 1.

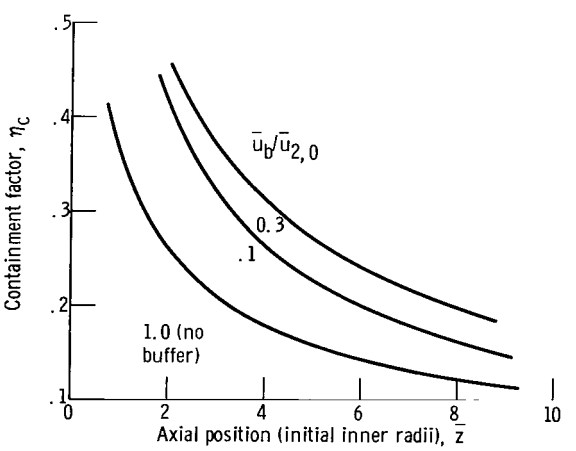

Figure 6. - Effect of buffer region on total mass of inner fluid in system of length z. Turbulent flow; $\bar{u}_{2,0} = 50$; buffer thickness, 1.

in figure 4, again for turbulent flow and an average outer- to inner-velocity ratio of 50. Figure 4(a) is for no buffer region, and figure 4(b) is for a buffer thickness of 1 jet radius at a buffer- to outer-velocity ratio of 0.3. The reduction in the rate at which the inner fluid is accelerated is clearly shown by a comparison of the constant-velocity lines for $\bar{u} = 5$ (fig. 4). The constant-velocity lines for $\bar{u} = 49$ show that farther downstream the higher velocity outer fluid begins to overcome the initial buffer effect.

Figure 4 shows the entire velocity field regardless of species and does not, therefore, clearly reflect what happens to the inner stream fluid. Figure 5 shows the axial variation of the radially averaged velocity of the inner fluid, still for turbulent flow and for a buffer thickness of 1 jet radius and an average initial-velocity ratio of 50. The effect of a buffer region is shown more clearly in figure 5 than by the centerline concentrations shown in figure 3. A buffer- to outer-velocity ratio of 0.3 reduces the rate of acceleration of the inner stream fluid. At a distance of 8 jet radii downstream, the presence of a buffer with a velocity ratio of 0.1 results in a higher velocity inner fluid than the case with no buffer region.

The influence of a buffer region on the average inner fluid velocity can be interpreted as an effect on the mean residence time of the inner fluid in a given length of channel. Thus, the effect of a buffer region can be expressed in terms of its effect on the total mass of inner fluid that is contained in a channel of length $\bar{z}$, compared with the maximum amount that could be present. This maximum would occur for slip flow and no radial diffusion. The ratio of the total amount of inner fluid present to that which would exist with no interaction between the two streams is then a sort of "containment efficiency", or containment factor. It represents the degree to which the inner stream fluid has been accelerated. It can vary from a maximum of 1.0 down to $1/\bar{\bar{u}}_{2,0}$, which would represent instantaneous acceleration of the inner stream fluid.

Figure 6 shows a plot of this containment factor η_c for various channel lengths $\bar{z}$, turbulent flow, a buffer thickness of 1 jet radius, and $\bar{\bar{u}}_{2,0} = 50$. Figure 6 shows the significant effect of a buffer region on the amount of inner stream fluid contained in a channel of length $\bar{z}$. For a system that is 4 jet radii in length, a buffer region with a buffer- to outer-velocity ratio of 0.3 increases the amount of inner fluid present from 18 percent without a buffer to 31 percent of the theoretical maximum. A buffer-velocity ratio of 0.1 yields a containment factor of 0.26.

Figures 7 and 8 show turbulent concentration fields for initial-velocity ratios of 10 and 100, respectively. Comparison of these figures with figure 2 (for $\bar{\bar{u}}_{2,0} = 50$) indicates that the effect of a momentum buffer is more pronounced at higher initial-velocity ratios, quantatively shown in succeeding figures.

For an initial-velocity ratio of 50, the ratio of turbulent to laminar viscosity is 830 with no buffer region; this value was used in the calculation illustrated in figure 2(a). With a buffer region present, a momentum-averaged velocity of the outer fluid yields a

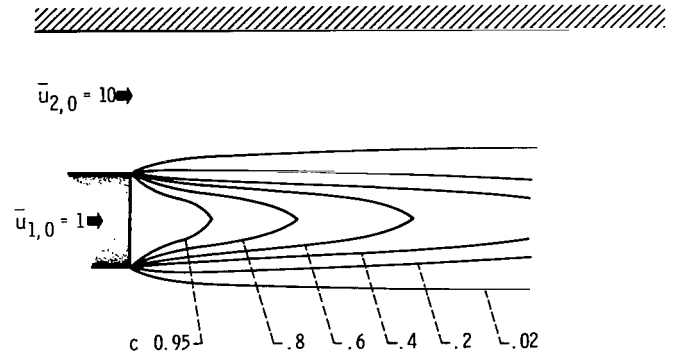

(a) No buffer.

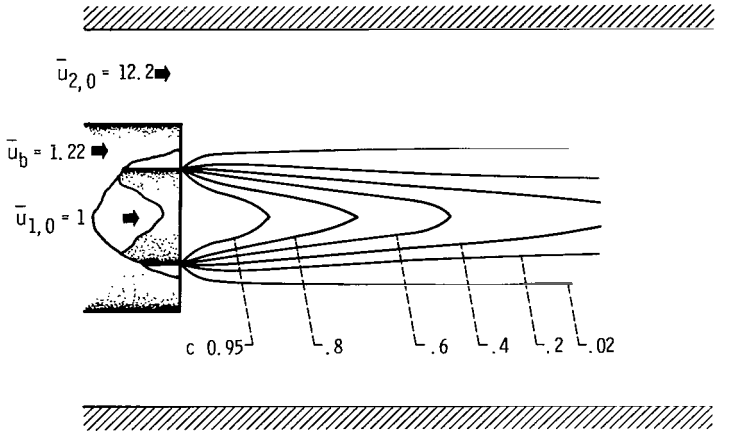

(b) Buffer thickness, 1; $\bar{u}_b/\bar{u}_{2,0} = 0.1$.

Figure 7. - Effect of buffer region on concentration field. Turbulent flow; $\bar{u}_{2,0} = 10$.

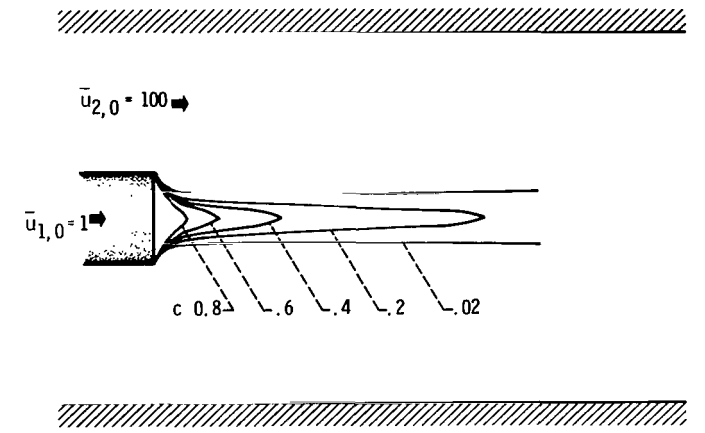

(a) No buffer.

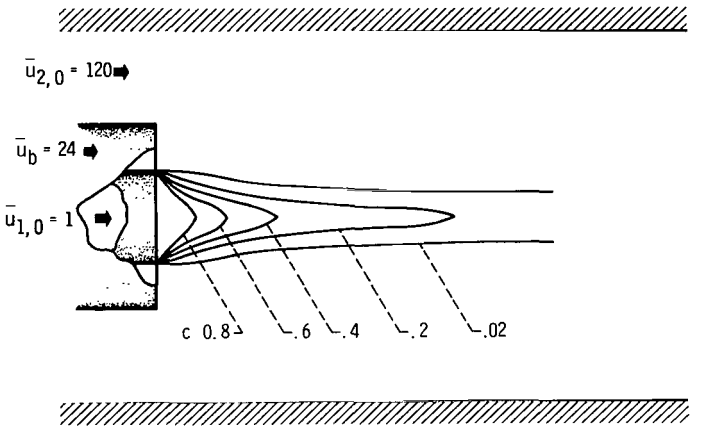

(b) Buffer thickness, 1; $\bar{u}_b/\bar{u}_{2,0} = 0.2$.

Figure 8. - Effect of buffer region on concentration field. Turbulent flow; $\bar{u}_{2,0} = 100$.

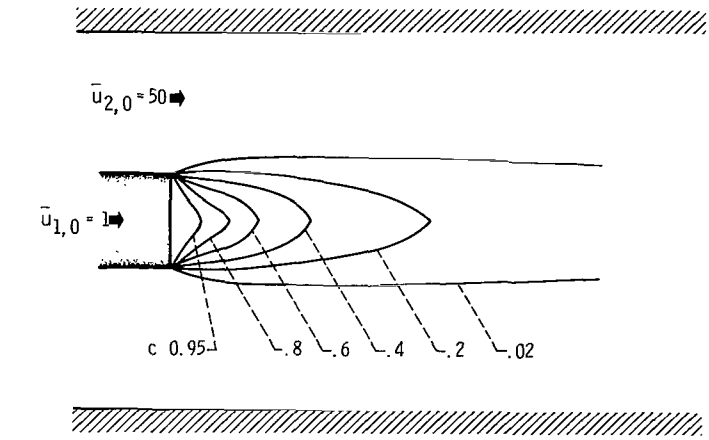

(a) No buffer region.

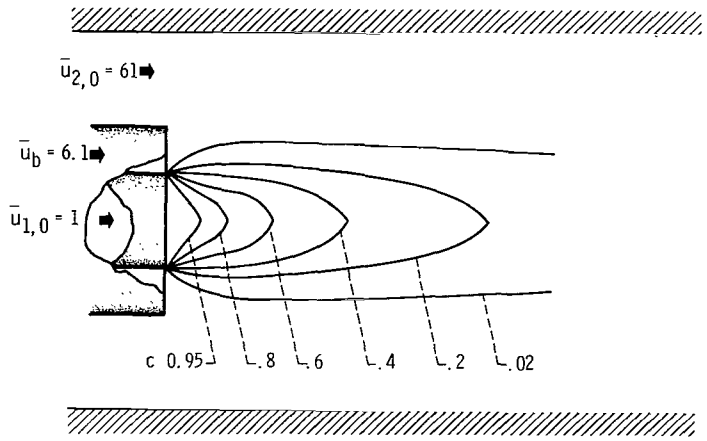

(b) Buffer thickness, 1; $\bar{u}_b/\bar{u}_{2,0} = 0.1$.

Figure 9. - Effect of buffer region on concentration field. Laminar flow; $\bar{u}_{2,0} = 50$.

value of 917 for $\rho\epsilon/\mu$ for the case shown in figure 2(b). Figures 9(a) and (b) show the corresponding concentration fields for laminar flow ($\rho\epsilon/\mu = 0$) for these two cases. A comparison of the concentration lines for $c = 0.2$ in figures 9(a) and (b) shows that a momentum buffer also has a considerable effect for laminar flow, as for turbulent flow, even though the general nature of the flow fields for laminar and turbulent mixing is markedly different.

Effect of Buffer Parameters on Containment Factors

Containment factors for laminar and turbulent flow are shown in figure 10 for basic coaxial mixing, with no buffer region present, and for initial-velocity ratios of 10, 50, and 100. As before, the containment factor is the ratio of the total mass of inner fluid contained in a duct of length $\bar{z}$ to the amount that would be present with no interaction between the two streams. This containment factor serves as a measure of the degree of stream mixing. Higher initial-velocity ratios, longer ducts, and the presence of turbulence all lead to increased mixing and lower containment factors.

The presence of a momentum buffer region reduces stream mixing and increases the containment factor. The effects of buffer-region thicknesses and velocities on the containment factor are shown in figure 11 for laminar flow and in figure 12 for turbulent flow. Curves are shown for buffer-region thicknesses of 0.5 to 1.0 jet radius and for initial-average-velocity ratios of 10, 50, and 100.

The curves exhibit the same general effect of buffer velocity on containment factor

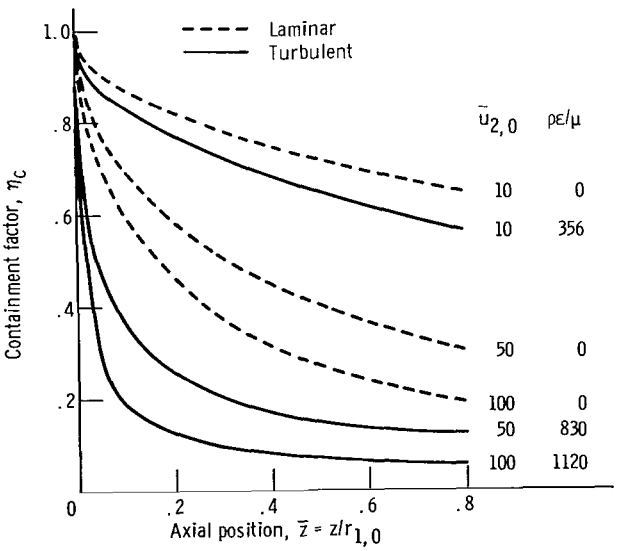

Figure 10. - Containment factors. No buffer region.

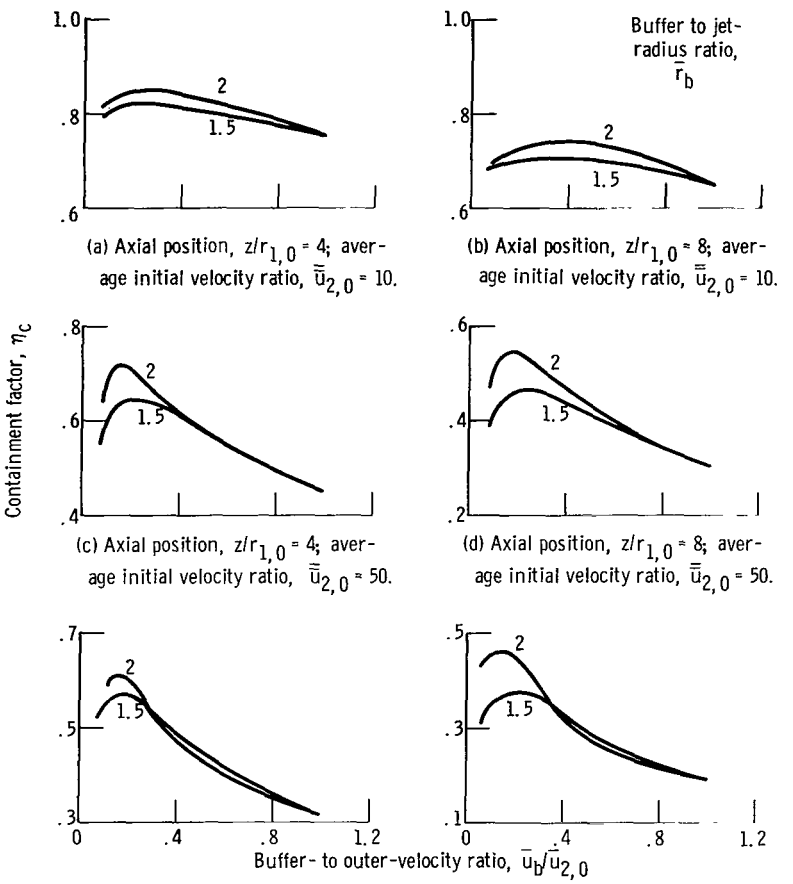

(a) Axial position, $z/r_{1,0} = 4$; average initial velocity ratio, $\bar{\bar{u}}_{2,0} = 10$.

(b) Axial position, $z/r_{1,0} = 8$; average initial velocity ratio, $\bar{\bar{u}}_{2,0} = 10$.

(c) Axial position, $z/r_{1,0} = 4$; average initial velocity ratio, $\bar{\bar{u}}_{2,0} = 50$.

(d) Axial position, $z/r_{1,0} = 8$; average initial velocity ratio, $\bar{\bar{u}}_{2,0} = 50$.

(e) Axial position, $z/r_{1,0} = 4$; average initial velocity ratio $\bar{\bar{u}}_{2,0} = 100$.

(f) Axial position, $z/r_{1,0} = 8$; average initial velocity ratio, $\bar{\bar{u}}_{2,0} = 100$.

Figure 11. - Buffer containment factors. Laminar flow.

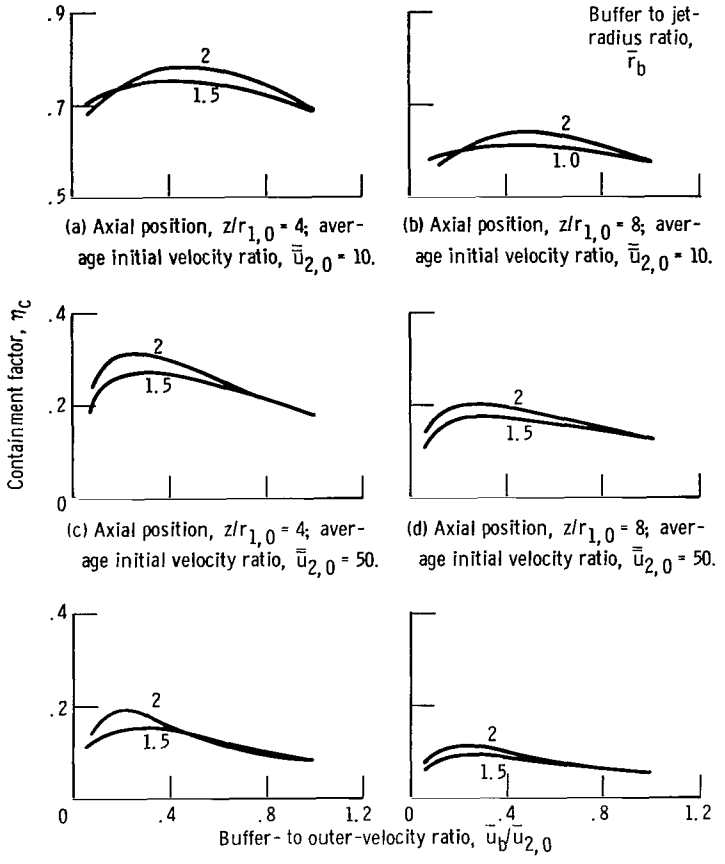

(a) Axial position, $z/r_{1,0} = 4$; average initial velocity ratio, $\bar{\bar{u}}_{2,0} = 10$.

(b) Axial position, $z/r_{1,0} = 8$; average initial velocity ratio, $\bar{\bar{u}}_{2,0} = 10$.

(c) Axial position, $z/r_{1,0} = 4$; average initial velocity ratio, $\bar{\bar{u}}_{2,0} = 50$.

(d) Axial position, $z/r_{1,0} = 8$; average initial velocity ratio, $\bar{\bar{u}}_{2,0} = 50$.

(e) Axial position, $z/r_{1,0} = 4$; average initial velocity ratio, $\bar{\bar{u}}_{2,0} = 100$.

(f) Axial position, $z/r_{1,0} = 8$; average initial velocity ratio, $\bar{\bar{u}}_{2,0} = 100$.

Figure 12. - Buffer containment factors. Turbulent flow.

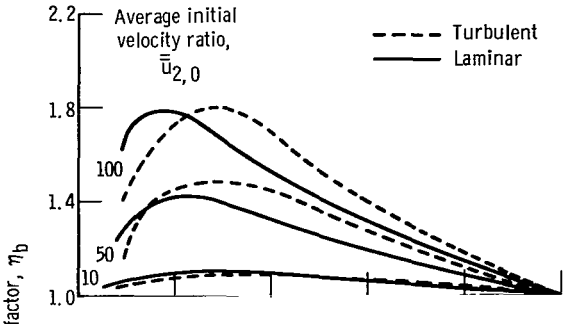

(a) Buffer- to jet-radius ratio, $\bar{r}_b = 1.5$.

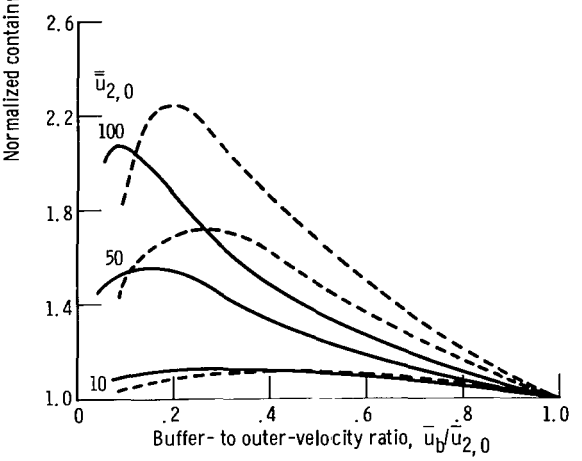

(b) Buffer- to jet-radius ratio, $\bar{r}_b = 2.0$.

Figure 13. - Normalized buffer containment factors for $z/r_{1,0} = 4$.

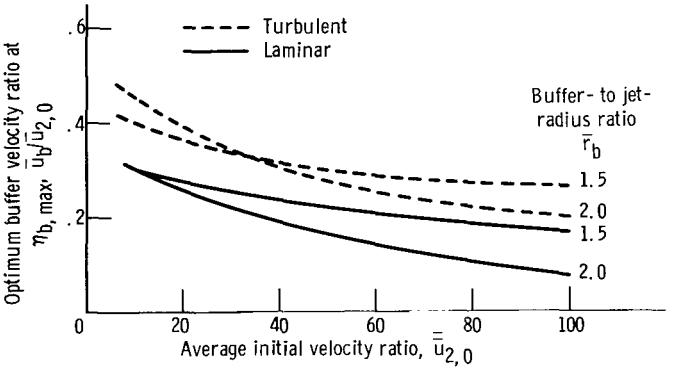

Figure 14. - Optimum-buffer to primary-velocity ratios for $z/r_{1,0} = 4$.

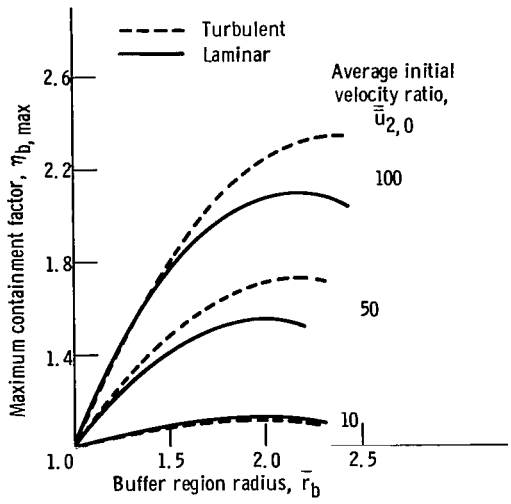

Figure 15. - Optimum buffer thicknesses for $z/r_{1,0} = 4$.

for laminar and turbulent flow. As the buffer-region velocity is decreased, the containment factor increases to a maximum value and then begins to decrease. A comparison of two corresponding curves for $\bar{z}$ values of 4 and 8 shows that the buffer effect is reduced for longer ducts, but that the optimum buffer- to outer-velocity ratio is essentially the same, at least at the higher initial-velocity ratios. The remaining results will be presented for a duct that is 4 jet radii in length ($\bar{z} = 4$).

It is difficult to assess the relative effects of a buffer region from the various curves of figures 11 and 12 because the absolute value of the containment factor is strongly affected by the initial velocity ratio and by the nature of the flow. It is therefore useful to normalize each curve to its value with no buffer region ($\bar{u}_b/\bar{u}_{2,0} = 1.0$).

The variation of such a normalized containment factor η_b with buffer- to outer-velocity ratio is shown in figure 13. The parameter η_b is the factor by which the amount of inner fluid in the duct has been increased by a buffer region. For an average-velocity ratio of 100, a buffer that is 1 initial jet radius thick ($\bar{r}_b = 2$), and turbulent flow, the amount of inner fluid in the duct is increased by a factor of more than 2 by decreasing the buffer-velocity ratio $\bar{u}_b/\bar{u}_{2,0}$ from 1 (no buffer) to 0.2. The maximum buffer effect is obtained for a buffer-velocity ratio of approximately 0.2, though there is some variation. Figure 14 shows the optimum buffer-velocity ratio as a function of the average-initial-velocity ratio $\bar{\bar{u}}_{2,0}$. For higher initial-velocity ratios, the optimum buffer-velocity ratio is lower. In general, the optimum buffer velocities range from 0.2 to 0.4 of the outer velocity for turbulent flow and from 0.1 to 0.3 for laminar flow. Thicker buffer regions require lower buffer velocities at moderate to high initial-velocity ratios.

Figure 15 shows the effect of the thickness of the buffer region on containment factors that have been maximized with respect to the buffer-velocity ratio. As with buffer-velocity ratio, an optimum exists. Higher initial-average-velocity ratios require somewhat thicker buffer regions, but the effect is relatively weak. For the range of conditions studied, the optimum momentum buffer thickness is approximately 1 jet radius. It is interesting to note that the optimum buffer thickness is virtually independent of whether the flow is laminar or turbulent.

CONCLUSIONS

The results of this study indicate some characteristics of two-component, three-region coaxial flow. All the calculations were carried out for a channel- to jet-radius ratio of 4 and for the following physical properties: a ratio of inner- to outer-fluid molecular weight of 100, an inner-fluid Schmidt number of 1, a ratio of outer- to inner-fluid viscosity of 0.2, and a ratio of outer- to inner-fluid molecular volume of 0.2. For laminar-flow calculations, the jet Reynolds number was taken as 200; for turbulent flow, the jet Reynolds number was taken to be 20 000. Channel lengths of 4 and 8 jet radii were considered, and buffer thicknesses of 0, 0.5, and 1 jet radius were investigated. Average ratios of outer- to inner-fluid initial velocity of 10, 50, and 100 were studied; for each of these cases, buffer- to outer-initial-velocity ratios of 0.1, 0.2, 0.3, and 0.4 were considered. For these ranges of conditions, the following results were obtained:

1. An optimum buffer-region velocity exists that minimizes the acceleration of the inner stream by the faster moving outer stream; this maximizes the amount of inner stream gas contained within a given length of the outer duct.

2. Similarly, there is an optimum buffer-region thickness.

3. The optimum buffer velocities range from 0.2 to 0.4 of the outer velocity for turbulent flow and from 0.1 to 0.3 for laminar flow.

4. The effect of a momentum buffer region is greater for higher ratios of outer- to inner-stream initial fluid velocity.

5. For a duct radius that is four times that of the jet, the optimum buffer thickness is 1 jet radius for both laminar and turbulent flow.

6. The presence of an intermediate-velocity momentum-buffer region of outer fluid significantly affects mass and momentum transfer and can increase the amount of inner fluid contained in a duct 4 jet radii in length by more than a factor of 2.

Lewis Research Center,
National Aeronautics and Space Administration,
Cleveland, Ohio, August 17, 1965.

REFERENCES

1. Libby, Paul A.: Theoretical Analysis of Turbulent Mixing of Reactive Gases With Application to Supersonic Combustion of Hydrogen. ARS J., vol. 32, no. 3, Mar. 1962, pp. 388-396.

2. Ferri, A.; Libby, P.A.; and Zakkay, V.: Theoretical and Experimental Investigation of Supersonic Combustion. High Temperatures in Aeronautics, C. Ferrari, ed., Pergamon Press, 1964, pp. 55-118.

3. Zakkay, Victor; Krause, Egon; and Woo, Stephen D. L.: Turbulent Transport Properties for Axisymmetric Heterogeneous Mixing. AIAA J., vol. 2, no. 11, Nov. 1964, pp. 1939-1947.

4. Alpinieri, Louis J.: Turbulent Mixing of Coaxial Jets. AIAA J., vol. 2, no. 9, Sept. 1964, pp. 1560-1567.

5. Weinstein, Herbert; and Todd, Carroll A.: A Numerical Solution of the Problem of Mixing of Laminar Coaxial Streams of Greatly Different Densities - Isothermal Case. NASA TN D-1534, 1963.

6. Ragsdale, Robert G.; and Weinstein, Herbert: On the Hydrodynamics of a Coaxial Flow Gaseous Reactor. Rept. No. TID-7653, pt. 1, AEC, 1963, pp. 82-88.

7. Ragsdale, Robert G.; Weinstein, Herbert; and Lanzo, Chester D.: Correlation of a Turbulent Air-Bromine Coaxial-Flow Experiment. NASA TN D-2121, 1964.

8. Sherwood, T. K.: Absorption and Extraction. McGraw-Hill Book Co., Inc., 1937, p. 18.

9. Schlichting, H.: Boundary Layer Theory. Fourth ed., McGraw-Hill Book Co., Inc., 1960, chs. XIX; XXIII.

10. Weinstein, Herbert; and Todd, Carroll A.: Analysis of Mixing of Coaxial Streams of Dissimilar Fluids Including Energy-Generation Terms. NASA TN D-2123, 1964.

11. Ragsdale, Robert G.; and Edwards, Oliver J.: Data Comparisons and Photographic Observations of Coaxial Mixing of Dissimilar Gases at Nearly Equal Stream Velocities. NASA TN D-3131, 1965.

"The aeronautical and space activities of the United States shall be conducted so as to contribute . . . to the expansion of human knowledge of phenomena in the atmosphere and space. The Administration shall provide for the widest practicable and appropriate dissemination of information concerning its activities and the results thereof."

—NATIONAL AERONAUTICS AND SPACE ACT OF 1958

NASA SCIENTIFIC AND TECHNICAL PUBLICATIONS

TECHNICAL REPORTS: Scientific and technical information considered important, complete, and a lasting contribution to existing knowledge.

TECHNICAL NOTES: Information less broad in scope but nevertheless of importance as a contribution to existing knowledge.

TECHNICAL MEMORANDUMS: Information receiving limited distribution because of preliminary data, security classification, or other reasons.

CONTRACTOR REPORTS: Technical information generated in connection with a NASA contract or grant and released under NASA auspices.

TECHNICAL TRANSLATIONS: Information published in a foreign language considered to merit NASA distribution in English.

TECHNICAL REPRINTS: Information derived from NASA activities and initially published in the form of journal articles.

SPECIAL PUBLICATIONS: Information derived from or of value to NASA activities but not necessarily reporting the results of individual NASA-programmed scientific efforts. Publications include conference proceedings, monographs, data compilations, handbooks, sourcebooks, and special bibliographies.

Details on the availability of these publications may be obtained from:

SCIENTIFIC AND TECHNICAL INFORMATION DIVISION

NATIONAL AERONAUTICS AND SPACE ADMINISTRATION

Washington, D.C. 20546